Asian Journal of Atmospheric Environment
Vol. 11, No. 3, pp. 153-164, September 2017
doi: https://doi.org/10.5572/ajae.2017.11.3.153
ISSN (Online) 2287-1160, ISSN (Print) 1976-6912

A CFD Study of Near-field Odor Dispersion around a Cubic Building from Rooftop Emissions

Sang Jin Jeong*

Department of Energy and Environmental Engineering, Kyonggi University, Suwon-si, Gyeonggi-do 16227, Republic of Korea

*Corresponding author. Tel: +82-31-249-9734, E-mail: sjjung@kyonggi.ac.kr

ABSTRACT

Odor dispersion around a cubic building from rooftop odor emissions was investigated using computational fluid dynamics (CFD). The Shear Stress Transport (here after SST) k-ω model in FLUENT CFD code was used to simulate the flow and odor dispersion around a cubic building. The CFD simulations were performed for three different configurations of cubic buildings comprised of one building, two buildings or three buildings. Five test emission rates were assumed as 1000 OU/s, 2000 OU/s, 3000 OU/s, 4000 OU/s and 5000 OU/s, respectively. Experimental data from wind tunnels obtained by previous studies are used to validate the numerical result of an isolated cubic building. The simulated flow and concentration results of neutral stability condition were compared with the wind tunnel experiments. The profile of streamline velocity and concentration simulation results show a reasonable level of agreement with wind tunnel data. In case of a two-building configuration, the result of emission rate 1000 OU/s illustrates the same plume behavior as a one-building configuration. However, the plume tends to the cover rooftop surface and windward facet of a downstream building as the emission rate increases. In case of a three-building configuration, low emission rates (<4000 OU/s) form a similar plume zone to that of a two-building configuration. However, the addition of a third building, with an emission rate of 5000 OU/s, creates a much greater odorous plume zone on the surface of second building in comparison with a two-building configuration.

Key words: CFD model, SST k-ω model, Odor dispersion, Cubic building, Rooftop emission

1. INTRODUCTION

A large number of industrial, institutional, university and hospital laboratories, as well as manufacturing facilities, emit a wide range of potentially harmful pollutants (e.g., toxic and odorous chemicals) from rooftop stacks to urban environments. Therefore, the dispersion of potential hazardous exhaust from these stacks is of great concern when addressing possible consequences of such releases on human health and safety, as well as the environment in the stack vicinity (Yassin, 2013). Among these pollutants, exposure to unpleasant odors is one of the most frequent causes of air quality complaints in both industrial and urban areas. Odor nuisance is most frequently associated with discontinuous emissions generated by restaurants, fast food outlets and bars, which may occur for short/prolonged times, occasionally or on a repetitive basis depending on the actual operating hours of the facility (Pettarin *et al*., 2015).

Once odors are emitted from a source, their transport, dispersion and fate in the environment is controlled by a complex interaction that depends on the strength of emissions, meteorological conditions, topographic features around the site, stack height and near-field buildings. Therefore, it is difficult to predict odor dispersion with certainty due to the complex interaction between atmospheric flow and flow around buildings.

Near-field pollutant dispersion in the built environment is characterized by the complex interaction of plumes with flow fields perturbed by building obstacles. The dispersion field consists of local emission sources and the dispersion of the emissions in nearby individual buildings and the surrounding neighborhood (Tominaga and Stathopoulos, 2016).

The main assessment tools in urban physics are field measurements, full-scale and reduced-scale laboratory measurements and numerical simulation methods including Computational Fluid Dynamics (CFD) (Blocken, 2015). In the past two decades, micro-scale Computational Fluid Dynamics (CFD) simulation has been widely used as an emerging analysis method for pollutant dispersion around buildings and in urban areas, sometimes in lieu of wind tunnel tests. The CFD simulation method consists of solving the transport (advection and diffusion) equation of concentration

based on the velocity field obtained from the Navier-Stokes equations. CFD can provide detailed information about the relevant flow and concentration variables throughout the calculation domain. However, it is difficult to implement various dispersion processes such as atmospheric stratification, buoyancy, chemistry etc. to the model, whereas they are easily applied to the operational models (Tominaga and Stathopoulos, 2013).

Odor dispersion in the atmosphere has been the subject of numerous investigations, while there has been less research done on odor dispersion around buildings. Odor dispersion under steady winds and constant emissions in the presence of few buildings has been evaluated using the Re-Normalization Group (RNG) k-ε model by Maizi *et al*. (2010). Dourado *et al*. (2014) presented a fluctuating plume model. However, the model appears to over-predict dispersion if compared to the wind tunnel data. In spite of the increasing number of applications based on dispersion models, this modeling approach has not yet been adequately validated to be confidently used for odor impact assessment. Moreover, we are not aware of applications of odor dispersion models to more complex urban environments (Pettarin *et al*., 2015).

The SST k-ω accounts for the principal turbulent shear stress and uses the across-diffusion term in the ω equation to blend both the k-ω model and k-ε model and to ensure that the model equations behave appropriately in both the near-wall and far-field zones. Thus, the SST k-ω model offers a superior simulation performance as compared with the individual k-ω and k-ε models (Menter *et al*., 2003). Recently, The SST k-ω model is increasingly being used to predict pollutant dispersion around barriers and isolated building (e.g., Kim and Jeong, 2015; Kim *et al*., 2014; Ramponi and Blocken, 2012; Lin *et al*., 2009).

In this respect, the aim of this paper is to investigate the influence of upstream rooftop odor emissions on near-field buildings. For this purpose, the CFD simulations were performed for three building cases, namely, an isolated cubic building, two cubic buildings and three cubic buildings, respectively. The SST k-ω model was used to simulate the flow and odor dispersion around cubic buildings in this study.

2. MATERIALS AND METHODS

2.1 Numerical Method

FLUENT CFD software (FLUENT ver.14, 2012) was used to simulate wind flow and odor dispersion around various configurations of cubic buildings. The Reynolds-averaged conservation equations for mass and momentum were used to simulate the processes of interest. Mass and momentum conservation equations are written as follows;

$$\frac{\partial u_i}{\partial x_j}=0 \tag{1}$$

$$\frac{\partial u_i}{\partial t}+u_j\frac{\partial u_i}{\partial x_j}=-\frac{1}{\rho}\frac{\partial p}{\partial x_i}+\frac{\mu}{\rho}\frac{\partial^2 u_i}{\partial x_j \partial x_j}-\frac{\partial}{\partial x_j}(\overline{u_i' u_j'})+g_i \tag{2}$$

where u_j is the velocity of j component, t is the time, x_j is the j coordinate, ρ is the air density, μ is the dynamic viscosity; g_i is the gravitational body force;

$$-\overline{u_i' u_j'}=-\frac{1}{\rho}\mu_t\left(\frac{\partial u_i}{\partial u_j}+\frac{\partial u_j}{\partial u_i}\right)-\frac{2}{3}k\delta_{ij} \tag{3}$$

is the Reynolds stress; μ_t is the turbulent viscosity.

The turbulence kinetic energy, k, and the specific dissipation rate, ω, are obtained from the following transport equations (FLUENT ver.14, 2012):

$$\frac{\partial}{\partial t}(\rho k)+\frac{\partial}{\partial x_i}(\rho k u_i)=\frac{\partial}{\partial x_j}\left(\Gamma_k\frac{\partial k}{\partial x_j}\right)+\tilde{G}_k-Y_k+S_k \tag{4}$$

and

$$\frac{\partial}{\partial t}(\rho\omega)+\frac{\partial}{\partial x_j}(\rho\omega u_j)$$
$$=\frac{\partial}{\partial x_j}\left(\Gamma_\omega\frac{\partial\omega}{\partial x_j}\right)+G_\omega-Y_\omega+D_\omega+S_\omega \tag{5}$$

In these equations, $\tilde{G}_k$ represents the generation of turbulence kinetic energy due to mean velocity gradients, G_ω represents the generation of ω, Γ_k and Γ_ω represent the effective diffusivity of k and ω, respectively. Y_k and Y_ω represent the dissipation of k and ω due to turbulence. D_ω represents the cross-diffusion term. S_k and S_ω are user-defined source terms.

2.2 Evaluation of Odor Intensity

Hydrogen sulfide (H_2S) was selected as an odorous fluid and was also presumed to flow along with clean dry air. According to Lin *et al*. (2009), the modeled fluid was defined as clean air and H_2S and its mass fraction at the odor source is defined as;

$$Y_s=\frac{O_{cg}\times m_{H2S}}{(P_a M/RT)+O_{cg}\times m_{H2S}} \tag{6}$$

where Y_s is the odor mass fraction at the inlet of the system boundary, which is the ratio of the odorous gas mass to that of the total air mass in 1.0 m^3 and is dimensionless P_a is the atmospheric pressure of 101,325 Pa at sea level, T the temperature in K; M the molecular weight of dry air or 0.028966 kg/mol; R is the universal gas constant of 8.31432 J/(mol·K); O_{cg} the odor

source concentration in OU/m^3, and m_{H2S} the mass of H_2S required to produce one odor unit, expressed as kg/OU, and $m_{H2S} = 7.0 \times 10^{-9}$ kg/OU. An odor unit (OU) is defined as the number of times an odorous air sample needs to be diluted with clean air to be no longer detectable by 50% of a team of panelists. This diluted concentration is also referred to as the threshold level (Lin *et al*., 2007).

The advection - diffusion (AD) module was applied to study the species transport process by analyzing the mass fraction of pollutants in the mixture. FLUENT analyzes the mass diffusion process based on the following equations (Riddle *et al*., 2004):

$$J_i = -\left(\rho D + \frac{\mu_t}{Sc_t}\right)\nabla y \tag{7}$$

where J_i is the diffusion flux of the mixture (kg/m^{2}s), ρ is the density of the mixture (kg/m^3), D is the mass diffusion coefficient of the pollutant in the mixture (m^2/s), y is the mass fraction of the pollutant (kg/kg), μ_t is the turbulent viscosity (kg·s/m). Sc_t is the Turbulent Schmidt number.

2.3 Computational Domain and Boundary Condition

Fig. 1 shows the computational domain and boundary conditions. The domain was conceived following the COST Action 732 (Franke *et al*., 2007) and AIJ (Tominaga *et al*., 2008) guidelines. Its dimensions are equal to 25H × 11H × 6H (H = 10 m is building height) in the streamwise (x), lateral (z) and vertical (y) directions, respectively. Atmospheric stability was fixed to be in a neutral condition in this study. To compare the experiments by Li and Meroney (1983) and to test the effect of the same building in streamwise direction, cubic building was selected in this study. The three kinds of building configurations used in this study are shown in Table 1. Each configuration has five different emission conditions, namely 1000 OU/s, 2000 OU/s, 3000 OU/s, 4000 OU/s and 5000 OU/s, respectively. So, simulation cases comprise a total of 15 cases. For all cases a single wind direction perpendicular to the building face was considered.

Inlet velocity profile of the horizontal wind velocity in a neutral stability condition is defined as (Pieterse and Harms, 2013);

$$u = \frac{u_*}{\kappa} ln \frac{z}{z_0} \tag{8}$$

As illustrated by Lin *et al*. (2007) the vertical profile of temperature can be defined as follows;

$$T(z) = -\gamma_d (z + z_s) + T_s \tag{9}$$

Where, $T(z)$ is the air temperature (K) at z, γ_d is the

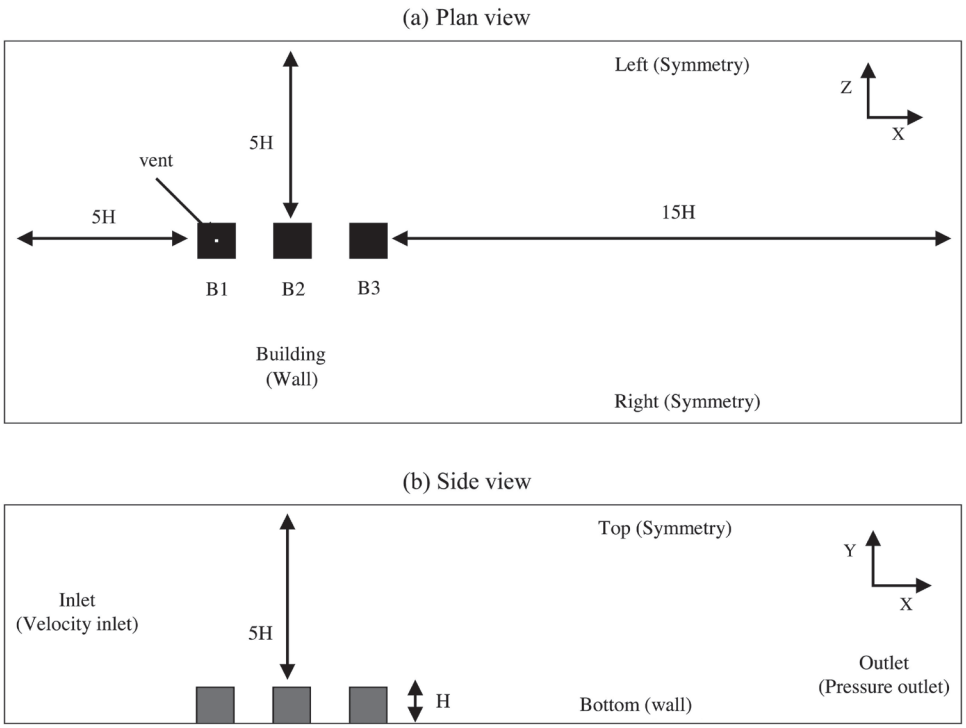

Fig. 1. Computational domain and boundary conditions.

Table 1. Building allocation of three different building configurations (where H = 10 m).

Case	Building configuration	Remark
I	B1 (Isolated building)	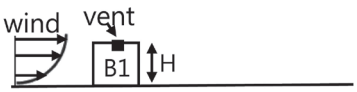
II	B1 and B2 downstream of B1	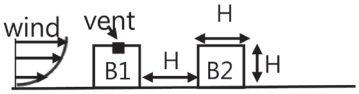
III	B1, B2 downstream of B1 and B3 downstream of B2	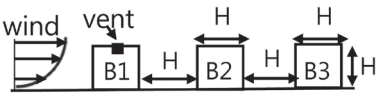

dry adiabatic lapse rate of 0.01 K/m. z_s is a height of 1.35 m above the earth's surface; T_s is the air temperature at z_s in K.

As presented in Pieterse and Harms (2013) the profile for the turbulent kinetic energy k and the turbulent dissipation of inlet ε for the neutral stratified atmospheric boundary layer is defined as follows;

$$k(z) = 5.48u_*^2 \tag{10}$$

$$\varepsilon(z) = \frac{u_*^3}{\kappa z} \tag{11}$$

3. QUALITY ASSESSMENT AND ASSURANCE STUDIES

3.1 Grid Sensitivity Study

In terms of overall grid resolution, Tominaga *et al*. (2008) advised a grid-convergence study until the prediction result does not change significantly any more with increasing grid resolution. To perform the grid sensitivity study, a one-building configuration case was selected. According to Blocken (2015), Franke *et al*. (2004) state that the grid should be fine enough to capture the important physical phenomena like shear layers and vortical structures with sufficient resolution. For urban and building models, they advise to use at least 10 cells per cube root of the building volume, and 10 cells in between every two buildings. So, three grids with cubical cells of 1.0, 0.5 and 0.4 m around building surfaces corresponding to cell counts of 10, 20 and 25 along the building height and facet were generated. Franke *et al*. (2004) advised to keep the stretching ratio below 1.3 in regions of high gradients, to limit the truncation error. Franke *et al*. (2004) also advised the use of hexahedral cells over tetrahedral cells, as hexahedral yield smaller truncation errors and better iterative convergence. To this end, outside the building block array an expansion ratio of 1.1 was applied to the cells resulting in final grids of 269,630, 664,000 and 938,720 hexahedral cells, respectively. The grid sensitivity study presented the comparison of the mean horizontal wind velocity U along vertical profiles at two locations with different flow regimes. The first profile (Fig. 2(a)) was located upstream of one building configuration; the second velocity profile (Fig. 2(b)) was located in the leeward wake region of a one-building configuration. As can be seen in Fig. 2, the profiles indicate some grid dependency, which becomes smaller on the finer grids. For both locations, very little quantitative differences are present between the 0.4 m-grid and the 0.5 m-grid whereas for the 1.0 m-grid in comparison to the 0.5 m-grid even qualitative differences are found. This suggests the 0.5 m-grid with a cell count of 20 per building height is appropriate for reliably predicting flows around an isolated cubic building.

3.2 Turbulent Schmidt Number Analysis

Gromke and Blocken (2015) state that the turbulent Schmidt number (Sct) is a fitting parameter, similar to the constants in turbulence models, which differs for different configurations. Studies on pollutant dispersion around isolated buildings using classical turbulence closure schemes for the Reynolds-averaged Navier-Stokes (RANS) equations suggest values for the Turbulent Schmidt number (here after Sc_t) ranging from 0.1 to 1.3 (Chavez *et al*., 2011; Blocken *et al*., 2008). According to Tominaga and Stathopoulos (2009), a smaller value of Sct such as 0.3 tends to provide better predictions of concentration distribution around plumes in open country and around a single building, where the turbulent momentum diffusion is often underestimated when using RANS models.

This variability suggests the need for careful consideration about the appropriate Sc_t number for each single study case. Therefore, pollutant dispersion around isolated cubic buildings was simulated with different values for Sc_t and validated against wind tunnel data in

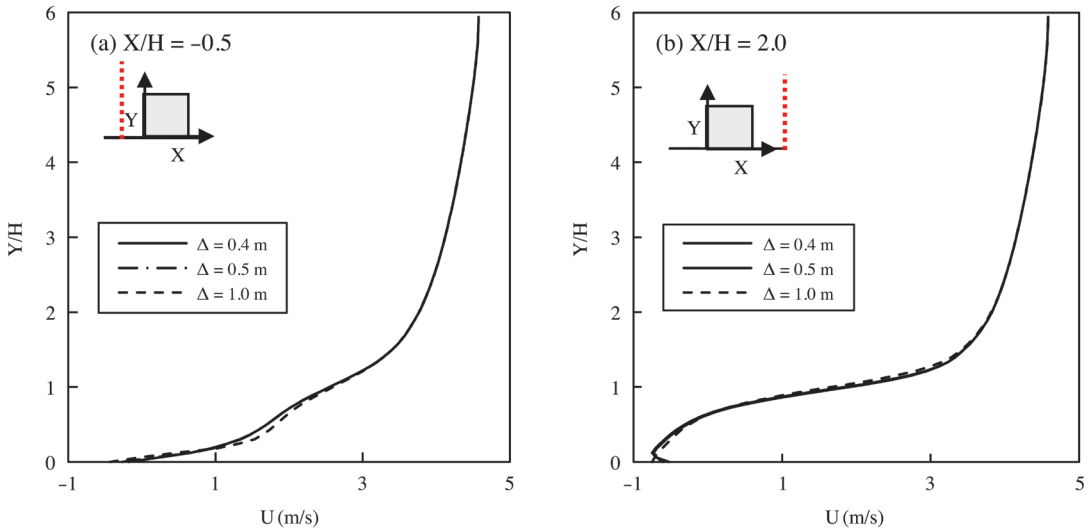

Fig. 2. Mean horizontal wind velocities U (m/s) on different grids at the upstream (a) and downstream wake region (b), Δ is mesh size, H (= 10 m) is building height. Vertical red dotted line shows the z-position.

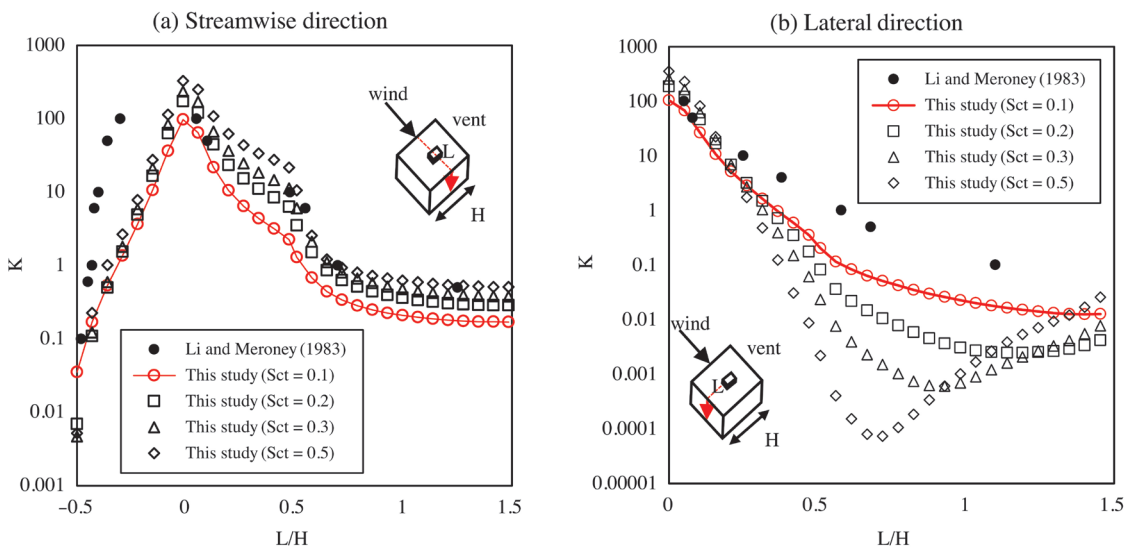

Fig. 3. Comparison of dimensionless concentration K on centerline of roof, leeward and sidewall.

this study.

Fig. 3 compares the contours of the dimensionless concentration, K, on the roof surface obtained with the present CFD and two experiments (Li and Meroney, 1983). In this study, dimensionless concentration K was defined as:

$$K = \frac{cH^2U_H}{Q_e} \tag{12}$$

where Q_e is the plume flow rate (m^3/s), c is mass fraction of tracer gas, H is the cube size (m), and U_H is mean x-velocity at building height. Although a higher Sc_t appears to provide a better prediction of the downwind dispersion along the rooftop centerline (Fig. 3(a)), there are no noticeable differences for the upwind dispersion. However, $Sc_t = 0.1$ produces a better result than other Sc_t results for the lateral direction (Fig. 3(b)). From this result, it can be concluded that $Sc_t = 0.1$ is the best number to use in this case.

3. 3 Assessment of the SST *k-ω* Turbulence Model

The next step of the quality assessment addresses the capability of the SST k-ω turbulence model to sim-

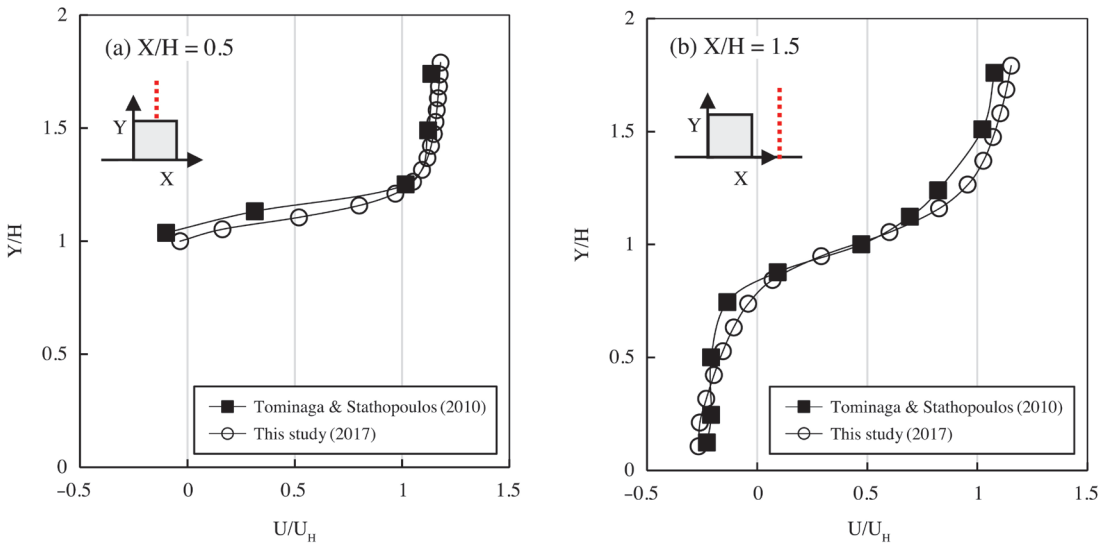

Fig. 4. Comparison of vertical distribution of streamwise velocity on (a) roof center (X/H = 0.5) and (b) behind cube (X/H = 1.5) at centerline.

ulate the flows around isolated buildings. Fig. 4 illustrates the comparison of vertical distribution of streamwise velocity on (a) roof center and (b) behind a cube at centerline. The simulated results showed a good agreement with the wind tunnel results.

4. EFFECTS OF DOWNSTREAM BUILDINGS ON FLOW AND ODOR DISPERSION

4.1 Effect of Downstream Building on Flow Field

In order to analyze the three different building configurations mentioned previously, a general view of the computational results in terms of velocity and stream line are illustrated in Fig. 5 and Fig. 6. This comparative view of results shows the difference of flow field behavior as the building number increases in the near-field environment. Additional buildings (B2 and B3) induce more low wind speed zones between buildings. These zones are also characterized by the presence of high velocity as can be shown by the streamlines in Fig. 6.

4.2 Influence of Odor Dispersion on Downstream Building

The Malodor Prevention Law recommends the air dilution sensory (ADS) test as a primary means to assess the level of odor pollution in dilution-to-threshold (D/T) ratios in South Korea (Kim, 2016). Under

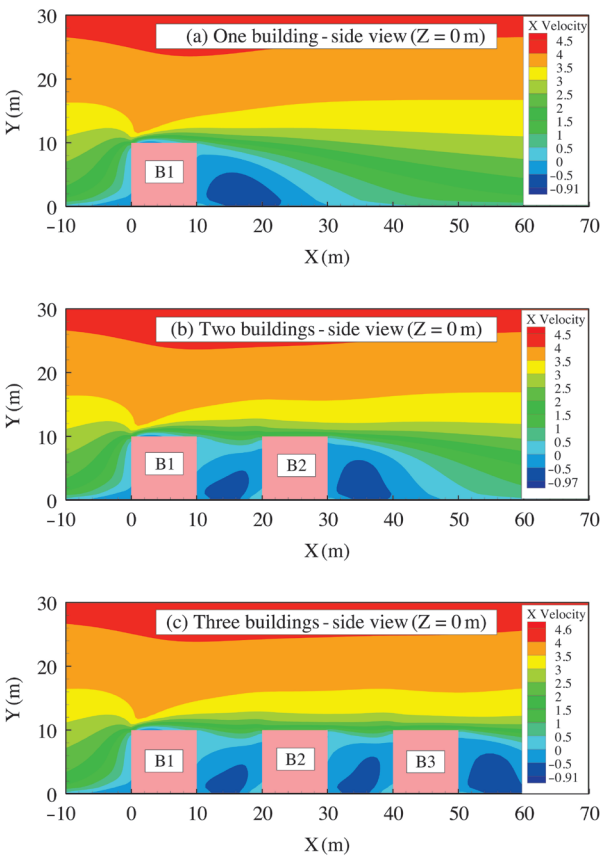

Fig. 5. Contours of x-velocity magnitude (m/s) for vent mass flow rate 1000 OU/s ($=7.0\times10^{-6}$ kg/s). (a) a one-building configuration, (b) a two-building configuration, (c) a three-building configuration.

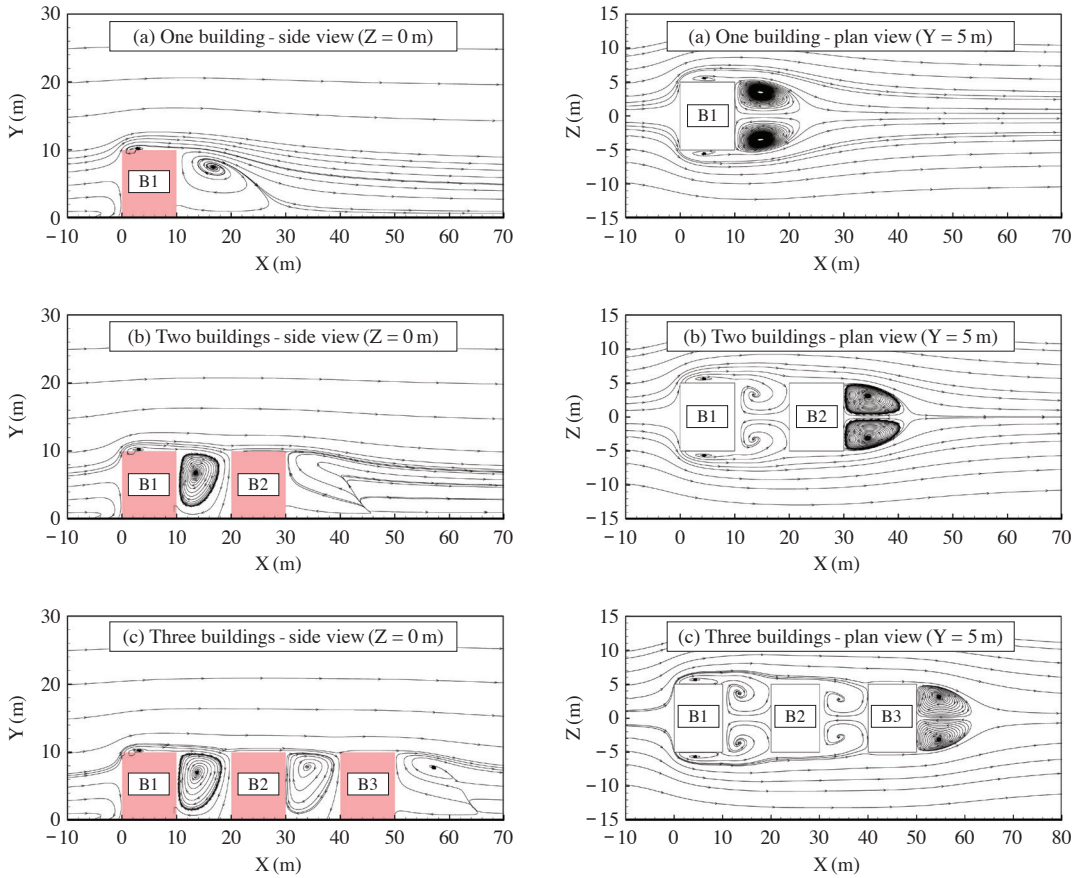

Fig. 6. Streamlines of vertical cross-section (Z = 0 m) and plan view at height Y = 5 m. (a) a one-building configuration, (b) a two-building configuration, (c) a three-building configuration.

this Law, samples are collected from the vents of odor sources and the emission limit is 1000 D/T (D/T is dilution-to-threshold (D/T) ratios) for facilities in industrial areas. Because values of D/T are theoretically comparable to OU/m^3 (Brancher *et al.*, 2017), 1000 OU/s was selected as the basic emission concentration in this study. Because 1 OU/m^3 is referred to as the threshold level (Lin *et al.*, 2007), 1 OU/m^3 is used to depict the size of an odorous plume zone.

Fig. 7 shows influencing area of the odorous plume zone for a one-building configuration. Overall, as the odor emission rate increases, the odor plume touched the rooftop surface and was dragged downstream of the building. When the emission rate is 3000 OU/s, most of the building's leeward facet is included in the odorous plume zone. However, most of the building's side facet is excluded from odorous plume zone.

Fig. 8 presents Influencing area of the odorous plume zone for a two-building configuration. Although an emission rate of 1000 OU/s illustrates the same plume behavior as a one-building configuration (Fig. 7(a)), it was noticed that the plume tends to the cover rooftop surface and windward facet of a downstream building as the emission rate increases to 2000 OU/s (Fig. 8(b)). Again, it was noticed that the side facet of the second building is included in the odorous plume zone at an emission rate of 4000 OU/s. The results clearly indicate that the increasing emission rate has a great impact on the second building.

Fig. 9 shows influencing area of the odorous plume zone of a three-building configuration. In general, it was observed that a low emission rate (< 4000 OU/s) has a similar odorous plume zone to that of a two-building configuration. However, the addition of a third building (B3), with an emission rate of 5000 OU/s, creates a much greater odorous plume zone on the surface of the second building in comparison with a two-building configuration. Therefore, most of the second building surface is covered with an odorous plume zone and the leeward facet of the third building is impacted by an odor plume at an emission rate of 5000 OU/s.

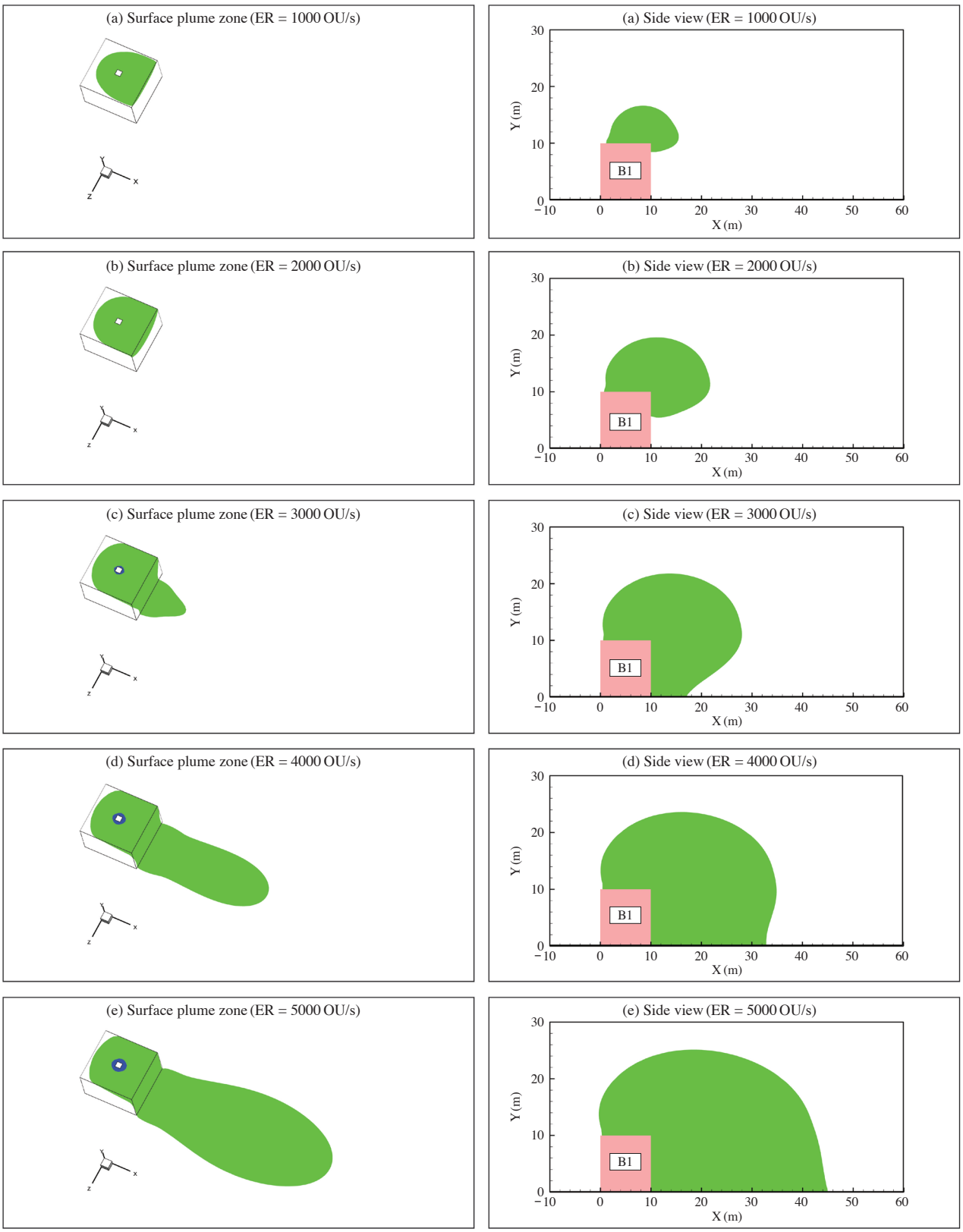

Fig. 7. Influencing area of the odorous plume zone (1 OU/m^3) for a one-building configuration. (a) 1000 OU/s, (b) 2000 OU/s, (c) 3000 OU/s, (d) 4000 OU/s, (e) 5000 OU/s.

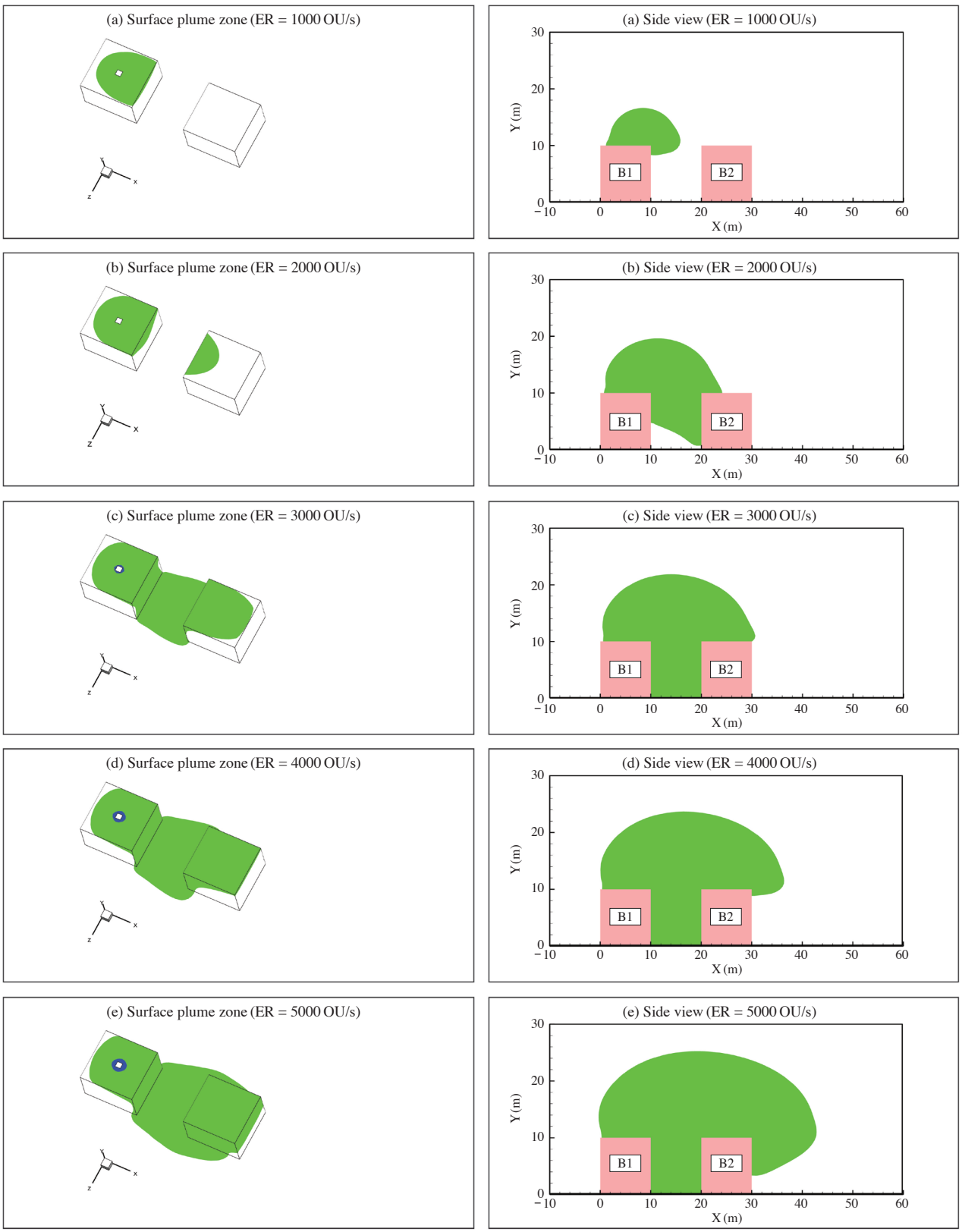

Fig. 8. Influencing area of the odorous plume zone (1 OU/m^3) for a two-building configuration. (a) 1000 OU/s, (b) 2000 OU/s, (c) 3000 OU/s, (d) 4000 OU/s, (e) 5000 OU/s.

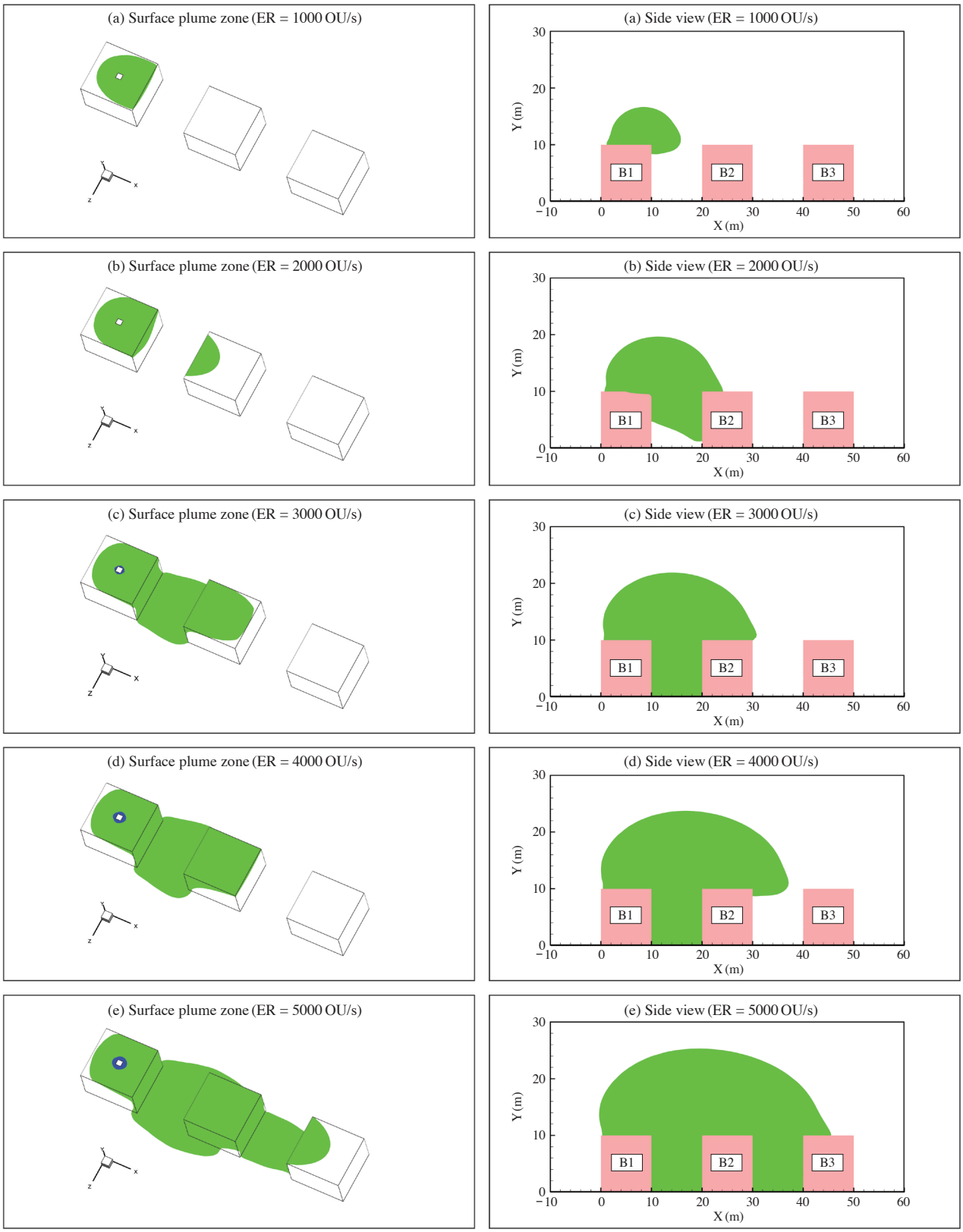

Fig. 9. Influencing area of the odorous plume zone (1 OU/m^3) for a three-building configuration. (a) 1000 OU/s, (b) 2000 OU/s, (c) 3000 OU/s, (d) 4000 OU/s, (e) 5000 OU/s.

5. CONCLUSION

The effect of downstream buildings on near-field odor dispersion from rooftop odor emissions was investigated using computational fluid dynamics (CFD). The simulated flow and concentration results of neutral stability condition were compared with the wind tunnel experiments. Although more comparisons are needed to derive firmer conclusions, this study has produced the following conclusions:

(1) The horizontal mean velocity simulation results of a one-building configuration showed a reasonable level of agreement with wind tunnel data.
(2) The result of the SST k-ω model with the Schmidt number $Sc_t = 0.1$ reveals good agreement with wind tunnel result for the concentration field.
(3) In the case of a one-building configuration, as the odor emission rate increases, the odor plume touched the rooftop surface and was dragged downstream of the building. However, some odor plume moves to the building's side facet but most of the odor plume moves to the building rooftop and leeward facet.
(4) In the case of a two-building configuration, the plume tends to cover the rooftop surface and windward facet of the downstream building as the emission rate increases. The results clearly indicate that the increasing emission rate has a great impact on the second building.
(5) In the case of a three-building configuration, the addition of a third building, with an emission rate of 5000 OU/s, creates a much greater odorous plume zone on the surface of the second building in comparison with a two-building configuration.

ACKNOWLEDGEMENT

This work was supported by Kyonggi University Research Grant 2015.

REFERENCES

Blocken, B. (2015) Computational Fluid Dynamics for urban physics: Importance, scales, possibilities, limitations and ten tips and tricks towards accurate and reliable simulations. Building and Environment 91, 219-245.

Brancher, M., Griffiths, K.D., Franco, D., Lisboa, H.M. (2017) A review of odour impact criteria in selected countries around the world. Chemosphere 168, 1531-1570.

Chavez, M., Hajra, B., Stathopoulos, T., Bahloul, A. (2011) Near-field pollutant dispersion in the built environment by CFD and wind tunnel simulations. Journal of Wind Engineering and Industrial Aerodynamics 99, 330-339.

Dourado, H., Santos, J.M., Reis, N.C. Jr., Mavroidis, I. (2014) Development of a fluctuating plume model for odour dispersion around buildings. Atmospheric Environment 89, 148-157.

FLUENT ver.14 (2012) User's Guide.

Franke, J., Hellsten, A., Schlünzen, H., Carissimo, B. (2007) Best practice guideline for the CFD simulation of flows in the urban environment. COST Action 732.

Franke, J., Hirsch, C., Jensen, A.G., Krus, H.W., Schatzmann, M., Westbury, P.S., Miles, S.D., Wisse, J.A., Wright, N.G. (2004) Recommendations on the use of CFD in wind engineering. In: van Beeck, J.P.A.J. (Ed.), Proceedings of the International Conference on Urban Wind Engineering and Building Aerodynamics, COST Action C14, Impact of Wind and Storm on City Life Built Environment. von Karman Institute, Sint-Genesius-Rode, Belgium. 5-7 May 2004.

Gromke, C., Blocken, B. (2015) Influence of avenue-trees on air quality at the urban neighborhood scale. Part I: Quality assurance studies and turbulent Schmidt number analysis for RANS CFD simulations. Environmental Pollution 196, 214-223.

Kim, A., Jeong, S.J. (2015) A study on the performance of a SST k-ω model for near field dispersion of odor from rooftop emission. Journal of Odor and Indoor Environment 14(2), 150-156.

Kim, K.H. (2016) The need for practical input data for modeling odor nuisance effects due to a municipal solid waste landfill in the surrounding environment. Environment International 87, 116-117.

Kim, K.J., Han, J.S., Gong, B.J., Jeong, S.J. (2014) Odor dispersion simulation around an isolated building using SST k-ω model. Journal of Odor and Indoor Environment 14(4), 263-269.

Li, W., Meroney, R.M. (1983) Gas dispersion near a cubical model building - Part I. Mean concentration measurements. Journal of Wind Engineering and Industrial Aerodynamics 12, 15-33.

Lin, X.J., Barrington, S., Choiniere, D., Prasher, S. (2007) Simulation of the effect of windbreaks on odour dispersion using the CFD SST k-ω model. Biosystems Engineering 98, 347-363.

Lin, X.J., Barrington, S., Choiniere, D., Prasher, S. (2009) Effect of weather conditions on windbreak odour dispersion. Journal of Wind Engineering and Industrial Aerodynamics 97, 487-496.

Maizi, A., Dhaouadi, H., Bournot, P., Mhiri, H. (2010) CFD prediction of odorous compound dispersion: Case study examining a full scale waste water treatment plant. BIOSYSTEMS ENGINEERING 106, 68-78.

Menter, F.R., Kuntz, M., Langtry, R. (2003) Ten years of industrial experience with the SST turbulence model. In: Hanjalic, K., Nagano, Y., Tummers, M. (Eds.), Tur-

bulence, Heat and Mass Transfer 4. Begell House Inc., Redding, CT, USA, pp. 625-632.
Pettarin, N., Campolo, M., Soldati, A. (2015) Urban air pollution by odor sources: Short time prediction. Atmospheric Environment 122, 74-82.
Pieterse, J.E., Harms, T.M. (2013) CFD investigation of the atmospheric boundary layer under different thermal stability conditions. Journal of Wind Engineering and Industrial Aerodynamics 121, 82-97.
Ramponi, R., Blocken, B. (2012a) CFD simulation of cross-ventilation for a generic isolated building: Impact of computational parameters. Building and Environments 53, 34-48.
Ramponi, R., Blocken, B. (2012b) CFD simulation of cross-ventilation for different isolated building configurations: Validation with wind tunnel measurements and analysis of physical and numerical diffusion effects. Journal of Wind Engineering and Industrial Aerodynamics 104-106, 408-418.
Riddle, A., Carruthers, D., Sharpe, A., McHugh, C., Stocker, J. (2004) Comparisons between FLUENT and ADMS for atmospheric dispersion modelling. Atmospheric Environment 38(7), 1029-1038.
Tominaga, Y., Mochida, A., Yoshie, R., Kataoka, H., Nozu, T., Yoshikawa, M., Shirasawa, T. (2008) AIJ guidelines for practical applications of CFD to pedestrian wind environment around buildings. Journal of Wind Engineering and Industrial Aerodynamics 96, 1749-1761.
Tominaga, Y., Stathopoulos, T. (2009) Numerical simulation of dispersion around an isolated cubic building: Comparison of various types of k-ε models. Atmospheric Environment 43, 3200-3210.
Tominaga, Y., Stathopoulos, T. (2010) Numerical simulation of dispersion around an isolated cubic building: Model evaluation of RANS and LES. Building and Environment 45, 2231-2239.
Tominaga, Y., Stathopoulos, T. (2013) CFD simulation of near-field pollutant dispersion in the urban environment: A review of current modeling techniques. Atmospheric Environment 79, 716-730.
Tominaga, Y., Stathopoulos, T. (2016) Ten questions concerning modeling of near-field pollutant dispersion in the built environment. Building and Environment 105, 390-402.
Yassin, M.F. (2013) A wind tunnel study on the effect of thermal stability on flow and dispersion of rooftop stack emissions in the near wake of a building. Atmospheric Environment 65, 89-100.

(Received 17 January 2017, revised 15 May 2017, accepted 14 June 2017)